

Looking through the pseudoscalar portal into dark matter: Novel mono-Higgs and mono-Z signatures at the LHC

Jose Miguel No*

Department of Physics and Astronomy, University of Sussex, Brighton BN1 9QH, United Kingdom
(Received 8 September 2015; published 5 February 2016)

Mono- X signatures are a powerful collider probe of the nature of dark matter. We show that mono-Higgs and mono- Z may be key signatures of pseudoscalar portal interactions between dark matter and the standard model. We demonstrate this using a simple renormalizable version of the portal, with a two-Higgs-doublet model as an electroweak symmetry breaking sector. Mono- Z and mono-Higgs signatures in this scenario are of resonant type, which constitutes a novel type of dark matter signature at the LHC.

DOI: [10.1103/PhysRevD.93.031701](https://doi.org/10.1103/PhysRevD.93.031701)

I. INTRODUCTION

The nature of dark matter (DM) is an outstanding mystery at the interface of particle physics and cosmology. The current DM candidate paradigm is the so-called weakly interacting massive particle (WIMP), a particle whose relic abundance is obtained via thermal freeze-out in the early Universe, and with a mass in the range GeV–TeV, around the scale of electroweak (EW) symmetry breaking $v = 246$ GeV. WIMP DM is very well motivated in connection with new physics close to the EW scale (see [1] for a review) and/or the existence of a hidden sector [singlet under the standard model (SM) gauge group] which interacts with the SM via a portal [2,3].

A large experimental effort aims to reveal the nature of (WIMP) DM and its interactions with SM particles, both indirectly by measuring the energetic particle product of DM annihilations in space, and directly by measuring the scattering of ambient DM from heavy nuclei. Current best limits on the spin-independent DM interaction cross section with nuclei by the large-underground-xenon (LUX) experiment [4] are very strong, particularly constraining for DM masses in the range 10–100 GeV. In contrast, limits on spin-dependent DM-nucleon interactions are much less stringent, generically favoring a pseudoscalar mediator of DM-nucleon interactions (which primarily yields spin-dependent interactions) over a scalar mediator. Such pseudoscalar mediated interactions generally lie well below the reach of present or upcoming DM direct detection experiments.

Direct or indirect probes of DM are complemented by searches at colliders, where pairs of DM particles could be produced. These escape the detector and manifest themselves as events showing an imbalance in momentum conservation, via the presence of missing transverse momentum \cancel{E}_T recoiling against a visible final state X . Searches for events with large \cancel{E}_T are a major activity at the Large Hadron Collider, precisely due to their (potential)

connection to DM [5]. Searches for DM in $X + \cancel{E}_T$ channels, referred to as mono- X , can be classified according to the nature of the visible particle(s) X . Experimental studies at the Tevatron and LHC have considered X as a hadronic jet [6–8], a photon γ [9,10], and W or Z bosons [11,12] and, after the discovery of the Higgs boson [13,14], they have also considered X to be the 125 GeV Higgs particle h [15]. Indeed, if DM is linked to the EW scale, W , Z and h signatures are natural places to search for it, with mono- W , Z , h having been recently considered as a paradigm for such potential signatures [16–23].

With the EW symmetry breaking sector being the most natural portal to a hidden sector, it is crucial to identify key probes of such portal interactions with the DM sector. As pseudoscalar portal interactions are significantly more difficult to probe experimentally via direct DM detection, collider probes constitute a rather unique window into these DM scenarios. I show that, for renormalizable pseudoscalar portal (known as axion portals) [24] scenarios, possible within extensions of the SM scalar sector, novel mono- W , Z , h signatures emerge with distinct kinematical features from other mono- X scenarios.

Such signatures generically occur in pseudoscalar DM portal scenarios if the mediator decays dominantly into DM, and they constitute a new LHC probe of DM, deeply linked to the realization of an extended Higgs sector in nature. In the following we explore them in detail using a simple and convenient two-Higgs-doublet-model (2HDM) realization of the pseudoscalar DM portal [25] as a simplified model [26], described in the next section.

II. DARK MATTER THROUGH THE PSEUDOSCALAR PORTAL

As a simple embedding of DM into the pseudoscalar portal scenario (see e.g. [25]), we consider DM to be a Dirac fermion ψ with mass m_ψ , coupling to a real singlet pseudoscalar mediator state a_0 via

$$V_{\text{dark}} = \frac{m_{a_0}^2}{2} a_0^2 + m_\psi \bar{\psi} \psi + y_\psi a_0 \bar{\psi} i \gamma^5 \psi. \quad (1)$$

*j.m.no@sussex.ac.uk

The minimal renormalizable realization of the pseudoscalar portal scenario [24] requires extending the SM Higgs sector to include two scalar doublets H_i ($i = 1, 2$). The scalar potential for the 2HDM reads

$$V_{2\text{HDM}} = \mu_1^2 |H_1|^2 + \mu_2^2 |H_2|^2 - \mu^2 [H_1^\dagger H_2 + \text{H.c.}] \\ + \frac{\lambda_1}{2} |H_1|^4 + \frac{\lambda_2}{2} |H_2|^4 + \lambda_3 |H_1|^2 |H_2|^2 \\ + \lambda_4 |H_1^\dagger H_2|^2 + \frac{\lambda_5}{2} [(H_1^\dagger H_2)^2 + \text{H.c.}] \quad (2)$$

where charge-parity (CP) conservation and a \mathcal{Z}_2 symmetry softly broken by μ are assumed. The pseudoscalar portal between the visible and hidden sectors occurs via [24,25]

$$V_{\text{portal}} = ika_0 H_1^\dagger H_2 + \text{H.c.} \quad (3)$$

The two doublets are $H_i = (\phi_i^+, (v_i + h_i + \eta_i)/\sqrt{2})^T$, with v_i the vacuum expectation value (vev) of the doublets ($\sqrt{v_1^2 + v_2^2} = v$ and $v_2/v_1 \equiv \tan \beta$). The scalar spectrum of the 2HDM contains a charged scalar $H^\pm = \cos \beta \phi_2^\pm - \sin \beta \phi_1^\pm$ and two neutral CP -even scalars $h = \cos \alpha h_2 - \sin \alpha h_1$, $H_0 = -\sin \alpha h_2 - \cos \alpha h_1$. We identify h with the 125 GeV Higgs state, which is SM-like in the limit $\beta - \alpha = \pi/2$ (see e.g. [28] for a review of 2HDM). For $\kappa \neq 0$, the would-be neutral CP -odd scalar $A_0 = \cos \beta \eta_2 - \sin \beta \eta_1$ mixes with a_0 through (3), yielding two pseudoscalar mass eigenstates a, A : $A = c_\theta A_0 + s_\theta a_0$, $a = c_\theta a_0 - s_\theta A_0$, with $c_\theta \equiv \cos \theta$ and $s_\theta \equiv \sin \theta$. We consider, in the following, the case in which the singletlike mediator a is lighter than A ($m_A > m_a$), and $m_a > 2m_\psi$ such that the decay $a \rightarrow \bar{\psi}\psi$ is possible. In terms of the mass eigenstates, the interactions (1) and (3) become

$$V_{\text{dark}} \supset y_\psi (c_\theta a + s_\theta A) \bar{\psi} i \gamma^5 \psi \\ V_{\text{portal}} = \frac{(m_A^2 - m_a^2) s_{2\theta}}{2v} (c_{\beta-\alpha} H_0 - s_{\beta-\alpha} h) \\ \times [aA(s_\theta^2 - c_\theta^2) + (a^2 - A^2) s_\theta c_\theta]. \quad (4)$$

Gauge interactions of the two doublets H_i yield the relevant interactions $aZh \propto s_\theta c_{\beta-\alpha}$, $AZh \propto c_\theta c_{\beta-\alpha}$, $aZH_0 \propto s_\theta s_{\beta-\alpha}$, $AZH_0 \propto c_\theta s_{\beta-\alpha}$, $aW^\pm H^\mp \propto s_\theta s_{\beta-\alpha}$, $AW^\pm H^\mp \propto c_\theta s_{\beta-\alpha}$, while $V = V_{2\text{HDM}} + V_{\text{dark}} + V_{\text{portal}}$ yields $aAh \propto s_{4\theta} s_{\beta-\alpha}$, $a\bar{\psi}\psi \propto c_\theta$ and $A\bar{\psi}\psi \propto s_\theta$.

Altogether, the interactions above lead to mono- h and mono- W, Z signatures at the LHC in various possible ways, which we discuss in detail in the next section. In particular, for $m_A > m_h + m_a$, $m_{H_0} > m_Z + m_a$, $m_{H^\pm} > m_{W^\pm} + m_a$, this scenario yields a novel signature: ‘‘resonant mono- h, W, Z ,’’ respectively, via the processes $pp \rightarrow A \rightarrow ha$, $pp \rightarrow H_0 \rightarrow Za$, $pp \rightarrow H^\pm \rightarrow W^\pm a$, with the mediator a subsequently decaying into DM.

III. MONO-HIGGS AND MONO- W, Z SIGNATURES AT THE LHC

As outlined above, in these scenarios there are two different kinds of processes which, through the production of $X + \bar{\psi}\psi$ ($X = W, Z, h$), lead to mono- X signatures at the LHC. Focusing on mono-Higgs for the purpose of illustration, there exist contributions from $pp(\bar{q}q) \rightarrow Z^* \rightarrow ha(a \rightarrow \bar{\psi}\psi)$ and $pp(gg) \rightarrow A \rightarrow ha(a \rightarrow \bar{\psi}\psi)$.

The former is similar to mono- h signatures arising in other simplified model scenarios [21–23] and has been discussed in detail in the literature (see e.g. [22]). These signatures are, however, generically suppressed by the presence of either an off-shell or a very massive particle in the s -channel. Together with the momentum transfer being cut off by the parton distribution functions, this leads to very small mono- h cross sections, making a mono- h signature difficult to probe at the 14 TeV run of the LHC, if it solely arises from this type of contribution.

In contrast, for $m_A > m_h + m_a$ the kinematics of the latter process is very different, due to A being resonantly produced. In this case, the 4-momentum of h and a is kinematically fixed, and E_T is bounded from above by

$$E_T^{\text{max}} = \frac{1}{2m_A} \sqrt{(m_A^2 - m_h^2 - m_a^2)^2 - 4m_h^2 m_a^2}. \quad (5)$$

The E_T distribution from this process is a steeply rising function with a sharp cutoff at E_T^{max} , a very distinct feature of these scenarios. At the same time, this contribution to mono- h is resonantly enhanced with respect to the former one, generically yielding a much larger cross section. Furthermore, it is important to stress that in this scenario the resonant contribution is proportional to $s_{\beta-\alpha}^2$ and thus maximal in the 2HDM alignment limit of a SM-like Higgs h (as favored by ATLAS and CMS analyses), whereas the off-shell contribution is proportional to $c_{\beta-\alpha}^2$, vanishing in that limit.

From here on, we perform a phenomenological analysis of resonant mono- h, Z signatures, choosing a type II 2HDM [28] benchmark $t_\beta = 3$, $c_{\beta-\alpha} = 0.05$ (close to the 2HDM alignment limit) and $m_{H^\pm} = m_{H_0} = m_A$ for simplicity [29], with $s_\theta = 0.3$, corresponding to a moderate mixing between the visible and dark sectors, and $y_\psi = 0.2$. For the mediator and DM masses we choose, respectively, $m_a = 80$ GeV, $m_\psi = 30$ GeV (which yield a DM annihilation cross section of order needed for a correct DM relic density [25]). In our scenario, $a \rightarrow \bar{\psi}\psi$ yields the dominant branching ratio (BR) of a if $y_\psi \gtrsim 0.02$, and $\text{BR}(a \rightarrow \bar{\psi}\psi) > 0.99$ for $y_\psi \gtrsim 0.1$. We stress that if the dominant BR of a is into DM states, then direct LHC searches for the mediator a decaying into visible SM particles will have a reduced sensitivity (see e.g. [30] for an analysis of such possible searches).

Before continuing, let us briefly comment on two important issues: First, since $y_\psi \gtrsim \mathcal{O}(0.01-0.1)$ for $a \rightarrow \bar{\psi}\psi$ to be the dominant decay mode of a , a sizable resonant mono- h signal amplitude depends on the interplay between $\text{BR}(A \rightarrow ah)$ and $\text{BR}(A \rightarrow \bar{\psi}\psi)$, which can be nontrivial as m_a , m_ψ and y_ψ vary. This issue is, however, not present for a resonant mono- Z signal. Second, resonant mono- h signatures may also occur in a pure 2HDM through the process $pp(gg) \rightarrow A \rightarrow hZ(Z \rightarrow \nu\nu)$. We stress that the phenomenology in the presence of the pseudoscalar portal to DM is radically different from that of the pure 2HDM: Contrary to the case of the DM portal, the interaction yielding a mono- h signature in the 2HDM vanishes for a SM-like Higgs h , as discussed above. Moreover, for a pure 2HDM the same process with $Z \rightarrow \ell\ell$ is a much more sensitive probe of the existence of A than the mono- h signature. This constitutes a generic, crucial way of disentangling a resonant $X + \cancel{E}_T$ signature where \cancel{E}_T originates in a dark sector (e.g. $a \rightarrow \bar{\psi}\psi$) from that where the \cancel{E}_T comes from $Z \rightarrow \nu\nu$, as the latter will have to be accompanied by a much more sensitive $Z \rightarrow \ell\ell$ counterpart, while the former will not.

In the following, taking as benchmark values $m_{H_0} = m_A = 300, 500, 700$ GeV (denoted, respectively, as benchmarks A, B, C), we discuss the existing bounds from the 8 TeV LHC run and explore the 14 TeV LHC run prospects for resonant mono- h , Z .

A. Mono-Higgs

Current ATLAS and CMS mono- h searches focus on the $h \rightarrow \gamma\gamma$ decay of the 125 GeV Higgs boson. For our analysis we use the selection criteria from the LHC 8 TeV run data analysis by ATLAS [15], which selects events with two photons with leading (subleading) transverse momentum $P_T^{\gamma\gamma} > 35(25)$ GeV, rapidity $|\eta^\gamma| < 2.37$, and in the invariant mass window $m_{\gamma\gamma} \in [105, 160]$ GeV. In addition, the photon pair is required to have been produced in association with a sizable amount of missing transverse momentum, $\cancel{E}_T > 90$ GeV, and such that $P_T^{\gamma\gamma} > 90$ GeV (to suppress background events where \cancel{E}_T is caused by mismeasurement of energies of identified physical objects). ATLAS yields a 95% C.L. upper bound on the cross section of 0.70 fb, while our 8 TeV signal samples for $m_A = 300, 500, 700$ GeV generated with MADGRAPH5_AMC@NLO [31,32], respectively, yield, after selection cuts, 0.143 fb, 0.043 fb and 0.011 fb, including next-to-leading-order (NLO) QCD effects computed using SUSHI [33].

In Fig. 1 we show the value of $\cancel{E}_T^{\text{max}}$ for resonant mono- h in the (m_A, m_a) plane, which highlights the fact that, while current searches are not sensitive to $m_A \lesssim 250$ GeV (as $\cancel{E}_T^{\text{max}} < 90$ GeV), the value of $\cancel{E}_T^{\text{max}}$ rapidly increases with m_A , making the signature $pp \rightarrow h\bar{\psi}\psi(h \rightarrow \gamma\gamma)$ promising for masses $m_A \gtrsim 300$ GeV at the LHC 14 TeV run. For our analysis of resonant mono- h prospects at LHC 14 TeV, we

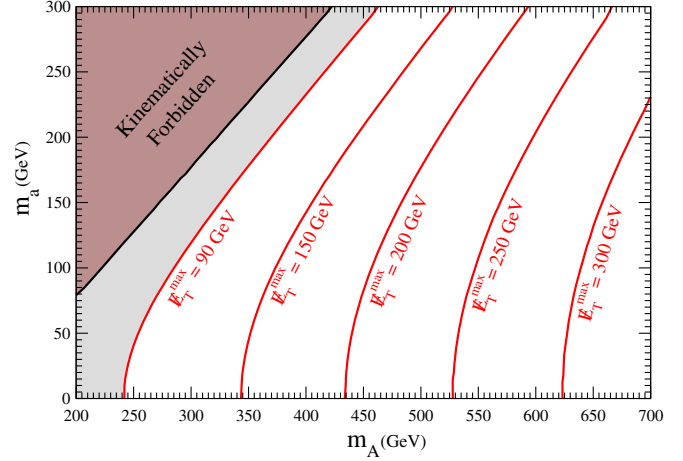


FIG. 1. Value of $\cancel{E}_T^{\text{max}}$ from (5) for resonant mono- h in the (m_A, m_a) plane. In the solid-brown region the decay $A \rightarrow ha$ is kinematically forbidden. The grey region lies below the event selection of [15]. A similar figure may be obtained in the plane (m_{H_0}, m_a) for resonant mono- Z .

generate our signal and background event samples with MADGRAPH5_AMC@NLO. These are passed on to PYTHIA [34] for parton showering and hadronization, and then to DELPHES [35] for a detector simulation. The main SM backgrounds are $Z\gamma\gamma$, $Z\gamma + \text{jets}$ (with a jet being misidentified as a photon, the fake rate being $P_{j \rightarrow \gamma} \sim 10^{-3}$ [36]) and SM Higgs associated production Zh , with $Z \rightarrow \nu\nu$. Backgrounds with a W instead of a Z boson may be suppressed by vetoing extra leptons. NLO cross section values are estimated via K -factors: $K \approx 1.65, 1.3$, respectively, for $Z\gamma\gamma$ and $Z\gamma + \text{jets}$ [37], $K \approx 1.3$ for Zh [38] and $K \approx 2.27, 1.8, 1.69$, respectively, for our signal benchmarks A, B, C through SUSHI.

In Table I I show the expected signal and background events for the LHC at 14 TeV with an integrated luminosity $\mathcal{L} = 300 \text{ fb}^{-1}$, after event selection and in the signal region. Event selection requirements for the two photon candidates follow [15] and are described above, dropping the $\cancel{E}_T > 90$ GeV cut. We subsequently define the signal region via $m_{\gamma\gamma} \in [120, 130]$ GeV and $\cancel{E}_T, P_T^{\gamma\gamma} > 80$ GeV, 180 GeV, 280 GeV, respectively, to maximize the sensitivity to

TABLE I. Expected number of events after event selection (see text for details) and signal region cuts for mono- h with $h \rightarrow \gamma\gamma$, for LHC 14 TeV with $\mathcal{L} = 300 \text{ fb}^{-1}$. Signal benchmarks A, B, C are described in Sec. III.

	A	B	C	Zh	$Z\gamma\gamma$	$Z\gamma j$
Event selection	249	56	16	51	517	157
$m_{\gamma\gamma} \in [120, 130]$ GeV	161	26	6	34	97	32
$\cancel{E}_T, P_T^{\gamma\gamma} > 80$ GeV	105	24	5	13	32	12
$\cancel{E}_T, P_T^{\gamma\gamma} > 180$ GeV	4	15	4	2	3	2
$\cancel{E}_T, P_T^{\gamma\gamma} > 280$ GeV	< 0.1	2	3	0.4	0.5	0.5

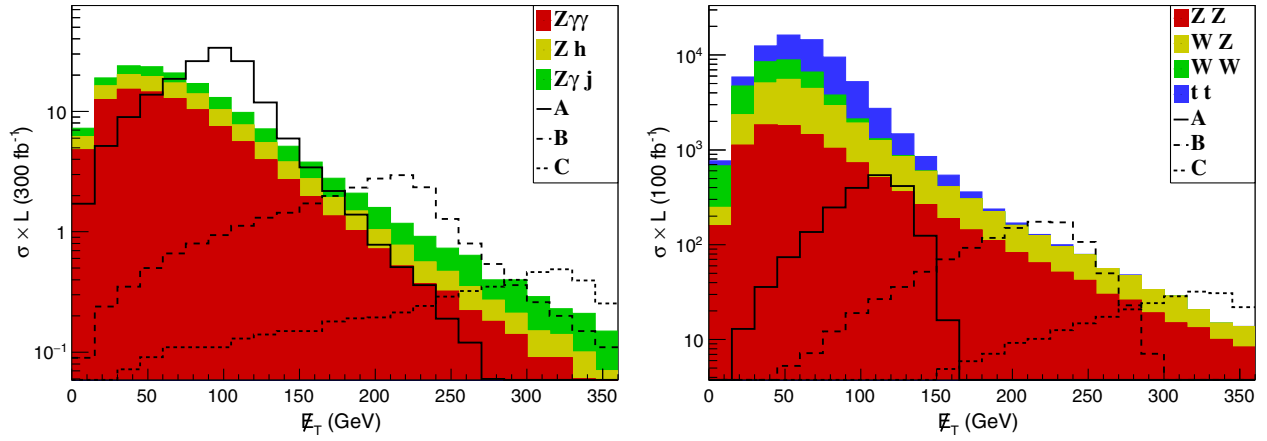


FIG. 2. Left panel: \cancel{E}_T distribution for mono- h signal benchmarks A (solid black line), B (dashed black line), C (fine-dashed black line) and background processes $Z\gamma\gamma$ (red), Zh (yellow) and $Z\gamma j$ (green), yielding $\cancel{E}_T + \gamma\gamma$, after event selection (see text for details) and for $m_{\gamma\gamma} \in [120, 130]$ GeV. Right panel: \cancel{E}_T distribution for mono- Z signal benchmarks A, B, C and background processes ZZ (red), WZ (yellow), WW (green) and $t\bar{t}$ (blue), yielding $\cancel{E}_T + \ell^+\ell^-$, after event selection (see text for details). In both cases, backgrounds are stacked on top of each other while signals are not, with bins being 15 GeV wide and normalized to show the number of events per bin.

benchmarks A, B, C. The \cancel{E}_T distribution for the three signal benchmarks and main backgrounds before applying this last cut is shown in Fig. 2 (left panel). From Table I, we see that, upon neglecting systematic uncertainties, an approximate significance $S/\sqrt{S+B} \sim 7.9, 3.2, 1.5$ is obtained in the signal region, respectively, for benchmarks A, B, C and $\mathcal{L} = 300 \text{ fb}^{-1}$.

B. Mono- Z

The recent ATLAS search [12] constrains mono- Z signatures with $Z \rightarrow \ell^+\ell^-$ using the available LHC 8 TeV run data. Their analysis selects events with two opposite sign (opposite charges) electrons or muons in the invariant mass window $m_{\ell\ell} \in [76, 106]$ GeV, with $P_T^\ell > 20$ GeV and rapidity $|\eta^\ell| < 2.5(2.47)$ for muons (electrons). The rapidity of the dilepton system has to satisfy $|\eta^{\ell\ell}| < 2.5$, and event selection further requires $\Delta\phi(\vec{\cancel{E}}_T, \vec{P}_T^{\ell\ell}) > 2.5$, $|P_T^{\ell\ell} - \cancel{E}_T|/P_T^{\ell\ell} < 0.5$. Four signal regions are defined, corresponding, respectively, to $\cancel{E}_T > 150$ GeV, 250 GeV, 350 GeV and 450 GeV. The ATLAS analysis yields a respective 95% C.L. observed upper bound on the cross section of 2.7 fb, 0.57 fb, 0.27 fb and 0.26 fb. Our three signal benchmark scenarios, A, B, C,

satisfy these bounds, and as we show in the following, they are very promising for the 14 TeV run of the LHC.

For our resonant mono- Z analysis at LHC 14 TeV, we follow a similar procedure to the one described for the mono- h case in the previous section, using MADGRAPH5_AMC@NLO, PYTHIA and DELPHES for our signal $pp \rightarrow Za$ ($Z \rightarrow \ell^+\ell^-$, $a \rightarrow \psi\psi$) and background event samples. The SM irreducible backgrounds are $ZZ \rightarrow \ell^+\ell^-\nu\bar{\nu}$ and $WW \rightarrow \ell^+\nu\ell^-\bar{\nu}$, while $WZ \rightarrow \ell\nu\ell^+\ell^-$ and $t\bar{t} \rightarrow b\ell^+\nu\bar{b}\ell^-\bar{\nu}$ are the most important reducible backgrounds. NLO cross sections are estimated via K -factors: $K \approx 1.2, 1.79, 1.68$, respectively, for ZZ, WZ and WW [39], $K \approx 1.5$ for $t\bar{t}$ [40] and $K \approx 2.36, 1.88, 1.75$, respectively, for our signal benchmarks A, B, C via SUSHI. Our event selection follows [12] and is discussed above, and we define three signal regions $\cancel{E}_T, P_T^{\gamma\ell} > 90$ GeV, 190 GeV, 290 GeV to respectively maximize sensitivity to benchmarks A, B, C.

In Table II we show the expected signal and background events for LHC at 14 TeV with an integrated luminosity $\mathcal{L} = 100 \text{ fb}^{-1}$, after event selection and in the various signal regions. Neglecting systematic uncertainties, an approximate significance $S/\sqrt{S+B} \sim 12.8, 18.7, 9.2$ is obtained in the respective optimal signal region for

TABLE II. Expected number of events after event selection (see text for details) and in the signal region for mono- Z with $Z \rightarrow \ell^+\ell^-$, for LHC 14 TeV with $\mathcal{L} = 100 \text{ fb}^{-1}$. Signal benchmarks A, B, C are described in Sec. III.

	A	B	C	ZZ	WW	WZ	$t\bar{t}$
Event selection	2009	1130	282	10100	12670	16680	32060
$\cancel{E}_T > 90$ GeV	1500	1105	279	2660	253	3530	5660
$\cancel{E}_T > 190$ GeV	4.5	733	254	414	< 0.1	357	30
$\cancel{E}_T > 290$ GeV	1.5	11	158	81	...	57	< 0.1

benchmarks A, B, C. In Fig. 2 (right panel), we show the \hat{E}_T distribution for signal and background after event selection.

Finally, although not discussed in this work, resonant mono- W signatures are also possible in this setup, but the suppressed production of H^\pm compared to A/H_0 makes them much less promising.

IV. DISCUSSION AND OUTLOOK

The previous analysis shows that resonant mono-Higgs and mono- Z are promising signatures for the 14 TeV run of LHC with $\mathcal{L} = 100\text{--}300 \text{ fb}^{-1}$, with mono- Z , in particular, being a very sensitive probe of pseudoscalar portal scenarios. Moreover, not only do these signatures constitute a window into the DM sector, but they are also potential discovery modes for the heavy states of the nonminimal scalar sector (here A, H_0), as their “usual” decay modes (e.g. in a pure 2HDM) will get suppressed by the presence of the new decay channels into the dark sector.

Finally, there are other possible avenues for exploring these pseudoscalar portal scenarios, like mono-jet searches on $pp(gg) > aj(a \rightarrow \bar{\psi}\psi)$, which we do not explore here, but will most certainly be complementary to the ones introduced in this work. One other aspect I have not explored is the possibility of a light a state, such that $m_h - m_Z > m_a > 2m_\psi$. The exotic Higgs decay $h \rightarrow Za \rightarrow \ell^+ \ell^- \bar{\psi}\psi$ is an interesting signature of such scenarios and will be studied elsewhere.

ACKNOWLEDGMENTS

I want to thank the organizers of the Les Houches 2015 Workshop “Physics at TeV Colliders” where this work began, and also Ken Mimasu, Veronica Sanz, Seyda Ipek and Belen Lopez-Laguna for very useful discussions. J. M. N. is supported by the People Programme (Marie Curie Actions) of the European Union Seventh Framework Programme (FP7/2007-2013) under REA Grant Agreement No. PIEF-GA-2013-625809.

-
- [1] G. Bertone, D. Hooper, and J. Silk, *Phys. Rep.* **405**, 279 (2005).
 - [2] R. Schabinger and J. D. Wells, *Phys. Rev. D* **72**, 093007 (2005).
 - [3] B. Patt and F. Wilczek, [arXiv:hep-ph/0605188](https://arxiv.org/abs/hep-ph/0605188).
 - [4] D. S. Akerib *et al.* (LUX Collaboration), *Phys. Rev. Lett.* **112**, 091303 (2014).
 - [5] D. E. Morrissey, T. Plehn, and T. M. P. Tait, *Phys. Rep.* **515**, 1 (2012).
 - [6] T. Aaltonen *et al.* (CDF Collaboration), *Phys. Rev. Lett.* **108**, 211804 (2012).
 - [7] V. Khachatryan *et al.* (CMS Collaboration), *Eur. Phys. J. C* **75**, 235 (2015).
 - [8] G. Aad *et al.* (ATLAS Collaboration), *Eur. Phys. J. C* **75**, 299 (2015).
 - [9] S. Chatrchyan *et al.* (CMS Collaboration), *Phys. Rev. Lett.* **108**, 261803 (2012).
 - [10] G. Aad *et al.* (ATLAS Collaboration), *Phys. Rev. Lett.* **110**, 011802 (2013).
 - [11] G. Aad *et al.* (ATLAS Collaboration), *Phys. Rev. Lett.* **112**, 041802 (2014).
 - [12] G. Aad *et al.* (ATLAS Collaboration), *Phys. Rev. D* **90**, 012004 (2014).
 - [13] G. Aad *et al.* (ATLAS Collaboration), *Phys. Lett. B* **716**, 1 (2012).
 - [14] S. Chatrchyan *et al.* (CMS Collaboration), *Phys. Lett. B* **716**, 30 (2012).
 - [15] G. Aad *et al.* (ATLAS Collaboration), *Phys. Rev. Lett.* **115**, 131801 (2015).
 - [16] F. J. Petriello, S. Quackenbush, and K. M. Zurek, *Phys. Rev. D* **77**, 115020 (2008).
 - [17] Y. Bai and T. M. P. Tait, *Phys. Lett. B* **723**, 384 (2013).
 - [18] N. F. Bell, J. B. Dent, A. J. Galea, T. D. Jacques, L. M. Krauss, and T. J. Weiler, *Phys. Rev. D* **86**, 096011 (2012).
 - [19] L. M. Carpenter, A. Nelson, C. Shimmin, T. M. P. Tait, and D. Whiteson, *Phys. Rev. D* **87**, 074005 (2013).
 - [20] A. Alves and K. Sinha, *Phys. Rev. D* **92**, 115013 (2015).
 - [21] A. A. Petrov and W. Shepherd, *Phys. Lett. B* **730**, 178 (2014).
 - [22] L. Carpenter, A. DiFranzo, M. Mulhearn, C. Shimmin, S. Tulin, and D. Whiteson, *Phys. Rev. D* **89**, 075017 (2014).
 - [23] A. Berlin, T. Lin, and L. T. Wang, *J. High Energy Phys.* **06** (2014) 078.
 - [24] Y. Nomura and J. Thaler, *Phys. Rev. D* **79**, 075008 (2009).
 - [25] S. Ipek, D. McKeen, and A. E. Nelson, *Phys. Rev. D* **90**, 055021 (2014).
 - [26] This renormalizable model has recently attracted significant attention as a possible explanation for the Galactic Center gamma ray excess [27] from DM annihilation [25].
 - [27] D. Hooper and L. Goodenough, *Phys. Lett. B* **697**, 412 (2011).
 - [28] G. C. Branco, P. M. Ferreira, L. Lavoura, M. N. Rebelo, M. Sher, and J. P. Silva, *Phys. Rep.* **516**, 1 (2012).
 - [29] We verify that our benchmarks satisfy EW precision observable constraints, and for each value of m_A we adjust μ in (2) to be within the region compatible with vacuum stability, perturbativity and unitarity.
 - [30] J. Fan, S. M. Koushiappas, and G. Landsberg, [arXiv:1507.06993](https://arxiv.org/abs/1507.06993).
 - [31] J. Alwall, M. Herquet, F. Maltoni, O. Mattelaer, and T. Stelzer, *J. High Energy Phys.* **06** (2011) 128.

JOSE MIGUEL NO

PHYSICAL REVIEW D **93**, 031701(R) (2016)

- [32] J. Alwall, R. Frederix, S. Frixione, V. Hirschi, F. Maltoni, O. Mattelaer, H.-S. Shao, T. Stelzer, P. Torrielli, and M. Zaro, *J. High Energy Phys.* **07** (2014) 079.
- [33] R. V. Harlander, S. Liebler, and H. Mantler, *Comput. Phys. Commun.* **184**, 1605 (2013).
- [34] T. Sjostrand, S. Mrenna, and P. Z. Skands, *Comput. Phys. Commun.* **178**, 852 (2008).
- [35] J. de Favereau, C. Delaere, P. Demin, A. Giammanco, V. Lemaître, A. Mertens, and M. Selvaggi (DELPHES 3 Collaboration), *J. High Energy Phys.* **02** (2014) 057.
- [36] J. Lilley, Report No. CERN-THESIS-2011-013.
- [37] J. M. Campbell, H. B. Hartanto, and C. Williams, *J. High Energy Phys.* **11** (2012) 162.
- [38] F. Maltoni, K. Mawatari, and M. Zaro, *Eur. Phys. J. C* **74**, 2710 (2014).
- [39] J. Ohnemus, *Phys. Rev. D* **50**, 1931 (1994).
- [40] M. L. Mangano, P. Nason, and G. Ridolfi, *Nucl. Phys.* **B373**, 295 (1992); G. Bevilacqua, M. Czakon, A. van Hameren, C. G. Papadopoulos, and M. Worek, *J. High Energy Phys.* **02** (2011) 083.